

the compounds by mass spectrometry. There was a difference in the relative distribution of the major sterol components (Table 1) of the experimental and control tissues throughout the 12 weeks of growth.

The reciprocal relation between campesterol and stigmasterol in the experimental and control tissues (Table 1) is of particular significance. In controls the ratio of campesterol to stigmasterol (C/S) was greater than 1 throughout the 12 weeks of growth, whereas in the experimental tissues the ratios were less than 1 during the 6- to 12-week periods. The C/S ratio in the 3-week-old experimental tissues was identical to that in the tissues at the outset of this experiment. Campesterol and stigmasterol appear to have no direct precursor-product relationship (11). Another major difference in the relative sterol composition of these tissues was the increased relative concentration of compound No. 6 (Table 1) of 17.1, 22.2, and 19.0 percent in the 3-, 6-, and 9-week-old control cultures, respectively, and the decrease to 2.5 percent in the 12-week cultures. A corresponding increase at 3, 6, and 9 weeks of this component did not occur in the experimental tissues. Upon preliminary examination of 12-week-old tobacco tissue cultures grown in contact with basalt materials found on Earth, no differences in the relative or absolute sterol concentrations of experimental and control tissues were noted.

When examined, the fatty acid constituents were identical to those previously reported for tobacco tissue cultures (15), and no qualitative differences were found between the experimental and control tissues. However, there were quantitative differences in relative and absolute fatty acid concentrations in the experimental and control tissues over the 12-week growth period.

In summary, greater total sterol concentrations were present in tobacco tissue cultures grown in contact with lunar material than in those grown without particulate material. The relative concentrations of phytosterols and their potential precursors were also significantly different. Absolute and relative differences in fatty-acid concentration also were found. No gross differences were apparent in the size or mass of the culture. These results are consistent with previous studies which show higher concentrations of pigment in similarly treated experimental tissues.

The findings of increased growth or pigment production for an algal species grown in contact with the lunar material returned by Apollo 11 (16) supports previous observations and the results presented here. The metabolic significance of the differences in relative and absolute sterol concentrations of the experimental and control tissues could not be explained from these data. The above data do, however, reflect the metabolic response by a sensitive plant system whose environment has been altered, presumably by available nutrients (2, 16) provided by lunar material.

JOHN D. WEETE

Lunar Science Institute,
Houston, Texas 77058

CHARLES H. WALKINSHAW

Forest Service,
U.S. Department of Agriculture, and
Lunar Receiving Laboratory,
National Aeronautics and Space
Administration, Houston, Texas 77058

JOHN L. LASETER

Department of Biological Sciences,
Louisiana State University,
New Orleans 70122

References and Notes

1. C. H. Walkinshaw, H. C. Sweet, S. Venkateswaran, W. H. Horne, *BioScience* **20**, 1297 (1970).
2. J. D. Weete and C. H. Walkinshaw, *Can. J. Bot.*, in press.
3. W. R. Morrison and L. M. Smith, *J. Lipid Res.* **5**, 600 (1964).
4. J. D. Weete, D. J. Weber, J. L. Laseter, *J. Bacteriol.* **103**, 536 (1970).
5. J. L. Laseter and J. D. Weete, *Science* **172**, 864 (1971).
6. B. A. Knights, *J. Gas Chromatogr.* **5**, 273 (1967).
7. P. S. Baur, personal communication.
8. W. W. Reid, *Phytochemistry* **7**, 451 (1968).
9. P. Benveniste, M. J. E. Hewlins, B. Fritig, *Eur. J. Biochem.* **9**, 526 (1969).
10. C. E. Cook, M. E. Twine, C. R. Tallent, I. Harper, G. Heunisch, J. B. Lewis, M. E. Wall, *Phytochemistry* **8**, 1025 (1969).
11. P. Benveniste, L. Hirth, G. Ourisson, *ibid.* **5**, 31 (1966).
12. B. Richardson, J. R. Baur, R. S. Halliwell, R. Langston, *Steroids* **11**, 231 (1968).
13. P. Benveniste, *Phytochemistry* **7**, 951 (1968).
14. ———, L. Hirth, G. Ourisson, *ibid.* **5**, 45 (1966).
15. J. D. Weete, *Lipids* **6**, 684 (1971).
16. M. P. Silverman, E. F. Munoz, V. I. Oyama, *Nature* **230**, 169 (1971).
17. We thank Debra Stakes and Carol Sherret for their technical assistance. This manuscript was prepared at the Lunar Science Institute under the joint support of the Universities Space Research Association and the Manned Spacecraft Center, NASA, Houston, Texas, under contract NSR 09-051-001 and at Louisiana State University at New Orleans under NASA contract NAS-9-11339. This is Lunar Science Institute Contribution No. 72.

28 October 1971; revised 21 December 1971 ■

Aragonite Crystals within Codiacean Algae:

Distinctive Morphology and Sedimentary Implications

Abstract. *Morphologic studies of single crystals of aragonite within Codiacean algae reveal characteristic crystal forms produced by two distinctly different modes of calcification. Diagnostic serrated crystals (1 micrometer in length) of aragonite originating within the extracellular sheaths of capitular filaments are incorporated into modern lime sediments and may serve as effective tracers for particles of algal origin. Intracellular calcification within *Penicillus dumetosus*, previously unreported, is represented by doubly terminated aragonite crystals ranging in size from 48 to 160 micrometers.*

The origin of both recent and ancient lime mud sediments has perplexed geologists for decades. Much attention has been focused on the origin of modern aragonitic lime mud inasmuch as it is believed to be the precursor of calcitic mud matrices found in ancient carbonate rocks. Physical breakage and abrasion of skeletal debris in agitated waters provides one mechanism for lime mud production (1). Extensive lime mud deposits found in relatively quiet sheltered waters, such as Florida Bay and the Great Bahama Bank, however, pose a different problem. These muds are characterized by an abundance of elongate single crystals of aragonite that are generally less than 15 μm .

Some workers (2, 3) believed this aragonite to be a nonskeletal, physico-

chemical precipitate; others (4) suggested the possibility of direct biochemical precipitation through the metabolic activity and decay of bacteria. An alternate hypothesis was proposed by Lowenstam (5) who reported the precipitation of prismatic aragonite "needles," 2 to 10 μm in length, as an integral skeletal component in several green algae and suggested algal disintegration products as a source of lime mud. Although some workers (3, 6) doubted the capability of algae to produce large quantities of lime mud, their potential as prolific producers of lime mud has been demonstrated (7) in the shallow marine waters of south Florida.

Within the 2- to 10- μm size fraction, it is virtually impossible to distinguish morphologically an aragonite "needle"

of algal origin from one precipitated directly from seawater. However, we have found other crystals of aragonite outside this size range within modern lime sediments that appear to be produced only by the calcifying green algae.

We have focused our attention primarily on the calcifying green alga *Penicillus dumetosus* (Lamouroux) Blainville (Fig. 1A), although other members of the Codiaceae, including *P. capitatus* Lamark, *Udotea*, and *Rhipocephalus*, were investigated also. Specimens used in this study were collected from Florida Bay and the nearshore shoals of the Atlantic adjacent to the Florida Keys. Living specimens of *P. capitatus* maintained in culture were examined also. Two distinct modes of calcification were found in the capitular filaments of *P. dumetosus*: extracellular and intracellular. Extracellular calcification in *Penicillus* is well known. Intracellular precipitation of aragonite, to the best of our knowledge, is reported here for the first time.

Extracellular calcification around the capitular filaments of *Penicillus* appears as a highly porous sheath (Fig. 1B). Studies by Marszalek (8) with the scanning electron microscope, have shown that this sheath is composed of aragonite crystals averaging $5.0\ \mu\text{m}$ in length and $0.3\ \mu\text{m}$ in width arranged in bundles that are oriented roughly parallel to the filament surface. Using the transmission electron microscope, we have found that this outer calcified sheath also contains at least two other crystal forms of considerably smaller size: (i) elongate prismatic crystals, generally $0.5\ \mu\text{m}$ in length by $0.07\ \mu\text{m}$ in width with planar to slightly curved terminations (Fig. 1D) and (ii) elon-

gate serrated crystals, approximately $1.0\ \mu\text{m}$ in length and $0.1\ \mu\text{m}$ in width, with a diagnostic "stair-step" pattern along their lateral margins (Fig. 1E).

We have observed both of these crystal forms in calcified capitular filaments of *P. dumetosus*, *P. capitatus*, *Udotea* sp., and *Rhipocephalus* sp. We have also examined bottom sediments from shallow water (less than 3 m) and sediment cores of mud banks from Florida Bay and have found aragonite crystals of identical morphology as common sedi-

mentary components within the lime mud fraction (Fig. 1F). If these crystals are unique to Codiacean algae, the $1\text{-}\mu\text{m}$ serrated crystals with their distinctive morphology (Fig. 1E) show particular promise for evaluating the relative contribution of algae to lime mud production, as well as for serving as sediment tracers in deep-sea sediments. Initial studies of bottom sediments collected from deeper waters surrounding the shallow St. Croix shelf have shown that these diagnostic ser-

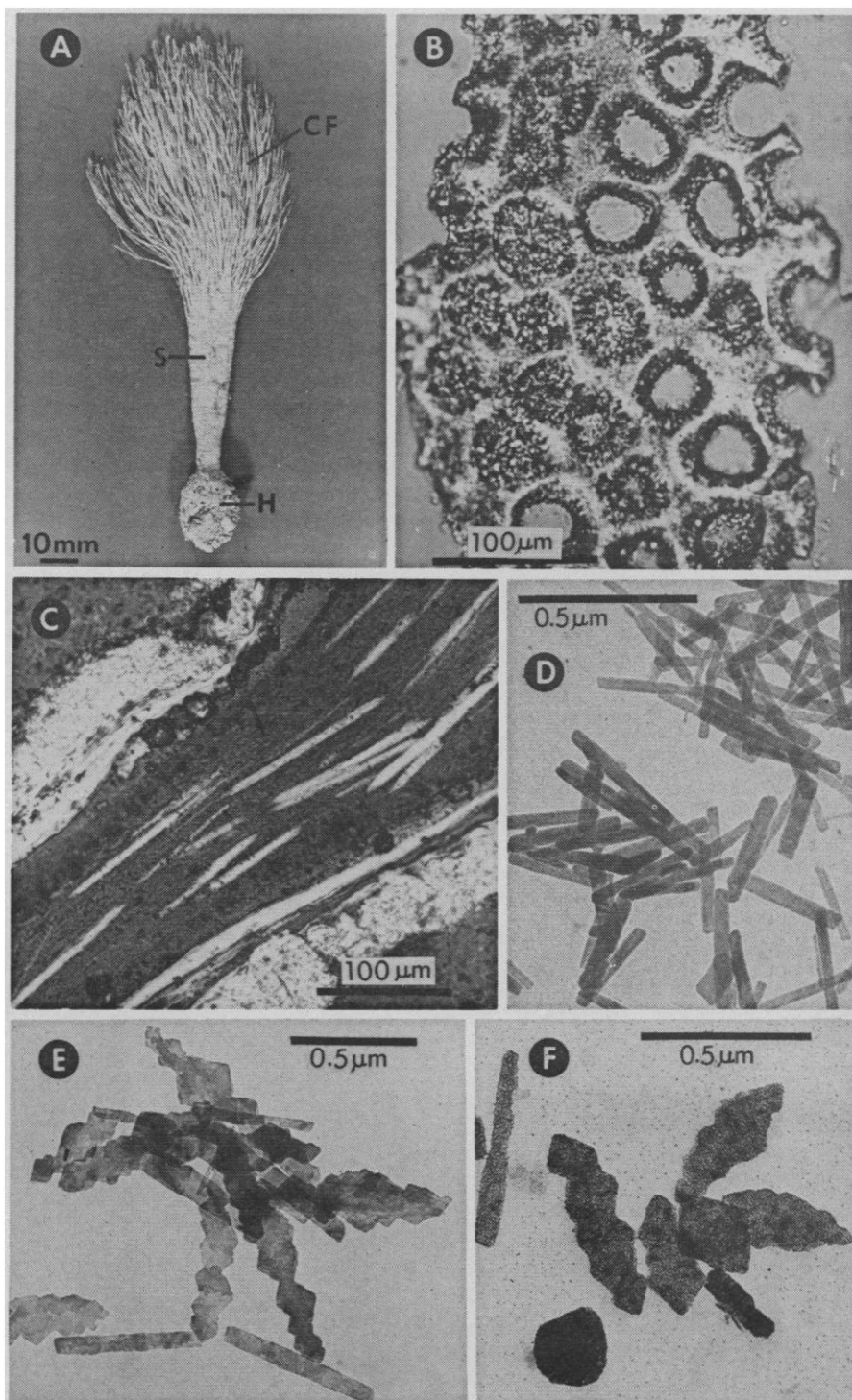


Fig. 1. (A) Whole specimen of *Penicillus dumetosus* showing holdfast (H), stalk (S), and tuft of capitular filaments (CF). (B) Fragment of the highly porous aragonitic sheath formed by extracellular calcification around the capitular filaments of *P. dumetosus*. (C) Longitudinal thin section, $30\ \mu\text{m}$ in thickness, of capitular filament of *P. dumetosus* showing doubly terminated aragonite crystals within the cytoplasm. Note extracellular aragonitic sheath adjacent to cytoplasm. (D) Electron micrograph of elongate aragonite prisms from the capitular filament sheath shown in (B). (E) Electron micrograph of diagnostic serrated crystals of aragonite from capitular filament sheath of *P. dumetosus*. (F) Electron micrograph of modern lime mud sediment from Florida Bay containing both elongate prismatic and serrated crystal forms of aragonite [compare with (D) and (E)].

rated crystals are present at depths as great as 675 m (9).

Intracellular calcification within the filaments of *P. dumetosus* is represented by elongate, doubly terminated aragonite crystals that average $94 \pm 33 \mu\text{m}$ in length with an observed range of 48 to $160 \mu\text{m}$ (Fig. 1C); these crystals range from 2 to $6 \mu\text{m}$ in width. Identification of these crystals as aragonite has been confirmed by electron diffraction of single crystals and by x-ray diffraction of crystal aggregates. That these crystals are intracellular in origin is shown (i) in thin sections of capitular filaments where crystals are contained entirely within the cytoplasm (Fig. 1C) and (ii) by isolation of the cytoplasm and its included crystals through decalcification of the extracellular sheath. These large (48 to $160 \mu\text{m}$) crystals of aragonite have been found only in *P. dumetosus* and may be of taxonomic value for the identification of this species. The presence of silt- to fine sand-sized, doubly terminated crystals of aragonite within lime sediments would possibly indicate a derivation from *P. dumetosus*.

RONALD D. PERKINS

Department of Geology,
Duke University,
Durham, North Carolina 27708

MICHAEL D. MCKENZIE*

Department of Botany

PATRICIA LURIE BLACKWELDER
Department of Zoology

References and Notes

1. R. K. Matthews, *J. Sediment. Petrology* **36**, 428 (1966).
2. T. W. Vaughn, *Geol. Soc. Amer. Bull.* **28**, 933 (1917); H. Gee, E. G. Moberg, D. M. Greenberg, R. Revelle, *Scripps Inst. Oceanogr. Bull. Tech. Ser.* **3**, 145 (1932); C. L. Smith, *J. Marine Res.* **3**, 147 (1940); P. E. Cloud and V. E. Barnes, *National Research Council Report, Treatise Marine Ecology and Paleontology No. 8* (1948), p. 29.
3. P. E. Cloud, *U.S. Geol. Surv. Prof. Pap. No. 350* (1962).
4. G. H. Drew, *Carnegie Inst. Wash. Publ. No. 182*, **5**, 7 (1914); C. B. Lipman, *ibid.* **No. 340**, **19**, 181 (1924); W. Bavendamm, *Ark. Mikrobiol.* **3**, 205 (1932); C. H. Openheimer, *Geochim. Cosmochim. Acta* **23**, 295 (1961); L. J. Greenfield, *Ann. N.Y. Acad. Sci.* **109**, 23 (1963).
5. H. A. Lowenstam, *J. Sediment. Petrology* **25**, 270 (1955).
6. N. D. Newell and J. K. Rigby, *Soc. Econ. Paleontol. Mineral. Spec. Publ.* **5**, 15 (1957).
7. K. W. Stockman, R. N. Ginsburg, E. A. Shinn, *J. Sediment. Petrology* **37**, 633 (1967).
8. D. S. Marszalek, *Proceedings of the Fourth Annual Scanning Electron Microscope Symposium*, Illinois Institute of Technology, Chicago (1971), p. 273.
9. S. C. Hastings, in preparation.
10. We thank K. M. Wilbur, R. B. Searles, and G. W. Lynts for helpful discussion and suggestions.

* Present address: Department of Oceanography, Texas A & M University, College Station 77843.

2 August 1971; revised 18 October 1971

Calcium Hydroxide: Its Role in the Fracture of Tricalcium Silicate Paste

Abstract. *The large areas of crystalline calcium hydroxide [Ca(OH)₂] formed during the hydration of tricalcium silicate (Ca₃SiO₅) correspond to low-porosity regions in the hydrated paste. During the early stage of hydration, areas between Ca(OH)₂ crystals which consist of Ca₃SiO₅ particles bonded together by calcium silicate hydrate represent the high-porosity portion of the paste. Because of the presence of Ca(OH)₂, fracture in the hardened paste during this period propagates preferentially through the areas bonded by the calcium silicate hydrate phase and around the Ca(OH)₂ crystals. Calcium hydroxide also acts as a crack arrester. The influence of Ca(OH)₂ on fracture diminishes with increased hydration.*

Although portland cement concrete is the most widely used man-made building material in the world, microstructural factors which control fracture propagation through the hydrated cement paste are not completely understood. Of the four major constituents that make up portland cement, the most important is tricalcium silicate (Ca₃SiO₅) which is often used as a simplified model system to enable one to gain an understanding of the mechanisms controlling the hydration and engineering properties of portland cement. The Ca₃SiO₅ reacts with water to form a poorly crystalline calcium silicate hydrate with high surface area and calcium hydroxide [Ca(OH)₂]. Calcium silicate hydrate is considered to be more important in controlling the engineering properties of the hydrated system than Ca(OH)₂ which occurs predominantly as large crystals, often covering an area of over 0.1 mm² each.

The large size of the Ca(OH)₂ crystals renders them easily observable by standard techniques of optical microscopy. The preparation and in situ hydration of Ca₃SiO₅ paste samples 40 μm thick at a ratio of water to solids (by weight) (w/s) of 0.4, which is in the range of w/s ratios used for studies of engineering properties, made it possible to fracture samples at various degrees of hydration and to study by optical microscopy the role of Ca(OH)₂ in the propagation of fracture through the hydrated system.

The Ca₃SiO₅ used in the study had a free lime content of < 0.1 percent (by weight) and a Blaine fineness of 4000 cm²/g (1). Samples were prepared by placing about 0.2 g of thoroughly mixed paste with a w/s ratio of 0.4 on a glass slide (7.6 by 2.5 by 0.16 cm). An identical slide was placed over the sample, and, by moving the two slides against one another, the paste was distributed evenly in a layer about 40 μm thick. Excess paste was removed,

and the slides were sealed at the edges with paraffin. The samples were stored in an environment having a relative humidity of 100 percent at $23^\circ \pm 2^\circ\text{C}$ until testing at 1, 3, 8, and 22 days.

Fracture was accomplished by three-point loading until failure occurred. Immediately after failure the sample, immersed in mineral oil to prevent drying, was studied by optical microscopy. Use of this technique ensured that the samples were fractured in a wet state and that the fracture pattern observed was due to mechanical stresses within the system rather than shrinkage.

The percentage of the total sample area covered by Ca(OH)₂ crystals at various degrees of hydration was determined by point counting. The reported Ca(OH)₂ areas include Ca₃SiO₅ particles, calcium silicate hydrate, and gel pores entrapped within the Ca(OH)₂ crystals (2).

Tricalcium silicate reacts with water to form "inner-product" and "outer-product" calcium silicate hydrate and Ca(OH)₂ (3). The outer-product calcium silicate hydrate and crystalline Ca(OH)₂ form outside the original boundary of the Ca₃SiO₅ grains, whereas the bulk of the calcium silicate hydrate occurs as inner product within the boundary of the original grain. Calcium hydroxide crystals grow around particles with which they come in contact. The particles entrapped within the Ca(OH)₂ crystals during the early stages of growth are only partially hydrated and may, indeed, never hydrate fully as they may be cut off from direct contact with the solution phase. At this stage the Ca(OH)₂ crystals are isolated from one another and represent low-porosity areas distributed throughout the groundmass. The space between the Ca(OH)₂ crystals is filled with Ca₃SiO₅ particles which continue to hydrate. The Ca₃SiO₅ particles are bound together by the outer-product calcium silicate hydrate which grows into the